A Novel Approach for Iris Encryption

Shrinivasrao B. Kulkarni
SDM College of Engg. and Technology
Department of CSE
Dharwad-580002,
Karnataka, India

Ravindra S. Hegadi
Karnataka University
Department of Computer Science
Dharwad-580001,
Karnataka, India

Umakant P. Kulkarni
SDM College of Engg. and Technology
Department of CSE
Dharwad-580002,
Karnataka, India

ABSTRACT
A biometric system provides automatic identification of an individual based on a unique feature or characteristic possessed by the individual. Iris recognition is one of such biometric systems and is regarded as the most reliable and accurate identification systems available. It is the process of recognizing a person by analyzing the random pattern of the iris [8]. It combines computer vision, pattern recognition, statistical inference, and optics. Its purpose is real-time, high confidence recognition of a person's identity by mathematical analysis of the random patterns that are visible within the iris of an eye[7][8]. The proposed system takes an image of the eye, detects the iris and extracts it. Then a binary image of the extracted iris is created in order to form an equivalent barcode. Similarly a test data is also processed into a barcode and is matched with the reference barcodes in the database [8]. Representation of iris as a barcode provides an efficient and encrypted way for storing the iris data and provides one more level of security.

Thus, the system has its application in various areas like national border controls: the iris can be used as a living passport, cell phone and other wireless-device-based authentication, secure access to bank accounts at cash machines, premises access control, credit-card authentication, Internet security, Biometric-Key Cryptography, etc[10].

Following parameters are observed. i.e. AR- Acceptance Ratio 58.90%. FRR- False Rejection Ratio 41.10%.FAR-False Acceptance Ratio 33.34 %. RR- Rejection Ratio 66.66%.

General Terms
Encryption, Algorithms, Performance, Design, Experimentation, Security, Human Factors, Verification.

Keywords
Aztec, Iris, Barcode, Recognition, Reed-Solomon, Barcode generation, Matching, Iris Encryption.

1. INTRODUCTION

1.1 Biometric Technology
A biometric system provides automatic recognition of an individual based on some sort of unique feature or characteristic possessed by the individual. Biometric systems have been developed based on fingerprints, facial features, voice, hand geometry, handwriting, the retina, and the one presented in this proposed work, the iris. Biometric systems work by first capturing a sample of the feature, such as recording a digital sound signal for voice recognition, or taking a digital color image for face recognition [3][7]. The sample is then transformed using some sort of mathematical function into a biometric template. The biometric template will provide a normalized, efficient and highly discriminating representation of the feature, which can then be objectively compared with other templates in order to determine identity.

1.2 The Human Iris
The iris is a thin circular diaphragm, which lies between the cornea and the lens of the human eye. A front-on view of the iris is shown in Figure 1. Due to the epigenetic nature of iris patterns, the two eyes of an individual contain completely independent iris patterns, and identical twins possess uncorrelated iris patterns [1].

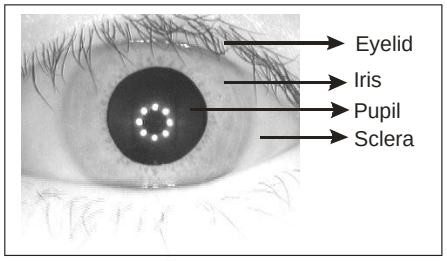

Figure 1: A front view of the iris

1.3 Iris Recognition
Image processing techniques can be employed to extract the unique iris pattern from a digitized image of the eye, and encode it into a biometric template, which can be stored in a database. This biometric template contains an objective mathematical representation of the unique information stored in the iris, and allows comparisons to be made between templates. When a subject wishes to be identified by the iris recognition system, their eye is first photographed, and then a template created for their iris region. This template is then compared with the other templates stored in a database until either a matching template is found and the subject is identified, or no match is found and the subject remains unidentified.

As compared with other biometric technologies, such as face, speech and finger recognition, iris recognition can easily be considered as the most reliable form of biometric technology[3][7].

2. RELATED WORK

2.1 Segmentation
The first stage of iris recognition is to isolate the actual iris region in a digital eye image. The iris region, shown in Figure 1, can be approximated by two circles, one for the iris/sclera boundary and another, interior to the first, for the iris/pupil boundary. The eyelids and eyelashes normally occlude the upper and lower parts of the iris region. Also, specular reflections can occur within the iris region corrupting the iris pattern [4]. A technique is required to isolate and exclude these artifacts as well as locating the circular iris region.

2.1.1 Daugman's Integro-differential Operator

Daugman makes use of an integro-differential operator for locating the circular iris and pupil regions, and also the arcs of the upper and lower eyelids. The integro-differential operator is defined as[3][7],

$$\max_{(r,x_p,y_o)} \left| G_\sigma(r) * \frac{\partial}{\partial r} \oint_{r,x_o,y_o} \frac{I(x,y)}{2\pi r} ds \right|$$

Where *I(x,y)* is the eye image, *r* is the radius to search for, $G_\sigma(r)$ is a Gaussian smoothing function, and *s* is the contour of the circle given by *r*, x_o, y_o . The operator searches for the circular path where there is maximum change in pixel values, by varying the radius and centre *x* and *y* position of the circular contour. The operator is applied iteratively with the amount of smoothing progressively reduced in order to attain precise localization. Eyelids are localized in a similar manner, with the path of contour integration changed from circular to an arc.

2.1.2 Eyelash and Noise detection

Eyelashes are treated as belonging to two types, separable eyelashes, which are isolated in the image, and multiple eyelashes, which are bunched together and overlap in the eye image. Separable eyelashes are detected using 1D Gabor filters, since the convolution of a separable eyelash with the Gaussian smoothing function results in a low output value. Thus, if a resultant point is smaller than a threshold, it is noted that this point belongs to an eyelash. Multiple eyelashes are detected using the variance of intensity. If the variance of intensity values in a small window is lower than a threshold, the centre of the window is considered as a point in an eyelash. Specular reflections along the eye image are detected using threshold, since the intensity values at these regions will be higher than at any other regions in the image [7].

2.2 Normalization

Once the iris region is successfully segmented from an eye image, the next stage is to transform the iris region so that it has fixed dimensions in order to allow comparisons [7].

2.2.1 Image Registration

The Wildes et al. system employs an image registration technique, which geometrically warps a newly acquired image $I_a(x,y)$, into alignment with a selected database image $I_d(x,y)$. When choosing a mapping function $(u(x, y), v(x, y))$ to transform the original coordinates, the image intensity values of the new image are made to be close to those of corresponding points in the reference image. The mapping function must be chosen so as to minimize

$$\int_x \int_y \left(I_d(x,y) - I_a(x-u, y-v)\right)^2 dxdy$$

while being constrained to capture a similarity transformation of image coordinates (x, y) to (x', y'), that is

$$\begin{pmatrix} x' \\ y' \end{pmatrix} = \begin{pmatrix} x \\ y \end{pmatrix} - sR(\emptyset) \begin{pmatrix} x \\ y \end{pmatrix}$$

with *s* a scaling factor and $R(\phi)$ a matrix representing rotation by ϕ. In implementation, given a pair of iris images I_a and I_d the wrapping parameters *s* and ϕ are recovered via an iterative minimization procedure.

2.3 Feature Encoding and Matching

In order to provide accurate recognition of individuals, the most discriminating information present in an iris pattern must be extracted. Only the significant features of the iris must be encoded so that comparisons between templates can be made. The template that is generated in the feature encoding process will also need a corresponding matching metric, which gives a measure of similarity between two iris templates[7].

2.3.1 Wavelet Encoding

Wavelets can be used to decompose the data in the iris region into components that appear at different resolutions. Wavelets have the advantage over traditional Fourier transform in that the frequency data is localized, allowing features which occur at the same position and resolution to be matched up. A number of wavelet filters, also called a bank of wavelets, is applied to the 2D iris region, one for each resolution with each wavelet a scaled version of some basis function [7]. The output of applying the wavelets is then encoded in order to provide a compact and discriminating representation of the iris pattern.

3. PROPOSED SYSTEM

The current system which we have proposed will include all the steps or conventional processes explained in Literature survey, but employs different techniques for each step. The major difference is the formation of barcodes, which is the main emphasis of this proposed work. Therefore, the various steps carried out are namely:

1. Architecture
2. Segmentation
3. Normalization
4. Feature Encoding
5. Barcode Generation
6. Matching

3.1 Architecture

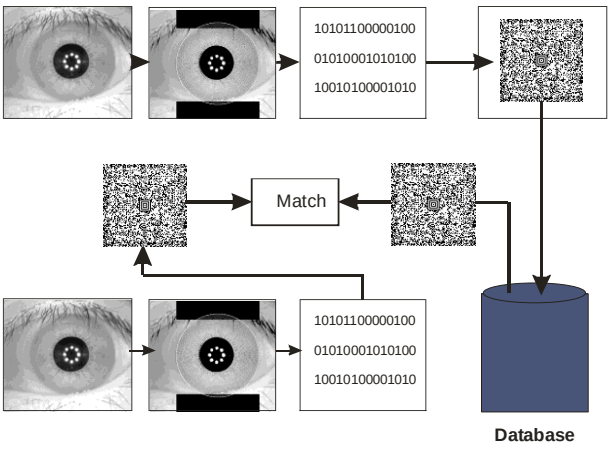

Figure 2: Architecture of Proposed System

3.2 Segmentation

3.2.1 Hough Transform

The Hough transform is a standard computer vision algorithm that can be used to determine the parameters of simple geometric objects, such as lines and circles, present in an image. The circular Hough transform can be employed to

deduce the radius and centre coordinates of the pupil and iris regions. Firstly, an edge map is generated by calculating the first derivatives of intensity values in an eye image and then thresholding the result. From the edge map, votes are cast in Hough space for the parameters of circles passing through each edge point [7]. These parameters are the centre coordinates x_c and y_c, and the radius r, which are able to define any circle according to the equation.

$$x_c^2 + y_c^2 = 0$$

A maximum point in the Hough space will correspond to the radius and centre coordinates of the circle best defined by the edge points. Wildes et al. and Kong and Zhang also make use of the parabolic Hough transform to detect the eyelids, approximating the upper and lower eyelids with parabolic arcs [9], which are represented as;

$$\left(-(x-h_j)sin\theta + (y-k_j)cos\theta\right)^2 = a_j(x-h_i)sin\theta + (y-k_j)cos\theta$$

where a_j controls the curvature, (hj, kj) is the peak of the parabola and θj is the angle of rotation relative to the x-axis.

In performing the preceding edge detection step, bias the derivatives in the horizontal direction for detecting the eyelids, and in the vertical direction for detecting the outer circular boundary of the iris, this is illustrated in Figure 3. The motivation for this is that the eyelids are usually horizontally aligned, and also the eyelid edge map will corrupt the circular iris boundary edge map if using all gradient data. Taking only the vertical gradients for locating the iris boundary will reduce influence of the eyelids when performing circular Hough transform, and not all of the edge pixels defining the circle are required for successful localization. Not only does this make circle localization more accurate, it also makes it more efficient, since there are less edge points to cast votes in the Hough space.

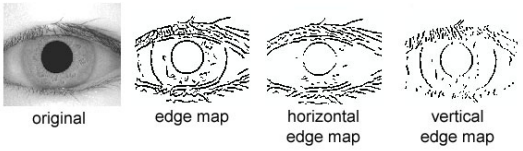

Figure 3: Eye image and its edge map after segmentation

3.3 Normalization

3.3.1 Daugman's Rubber Sheet Model

The homogenous rubber sheet model devised by Daugman remaps each point within the iris region to a pair of polar coordinates (r,θ) where r is on the interval [0,1] and θ is angle [0,2π].

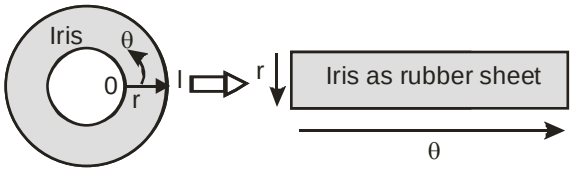

Figure 4: Daugman's rubber Sheet Model

The remapping of the iris region from (x,y) Cartesian coordinates to the normalized non-concentric polar representation is modeled as

$$I\big(x(r,\theta), y(r,\theta)\big) \rightarrow I(r,\theta)$$

With

$$x(r,\theta) = (1-r)x_p(\theta) + rx_j(\theta) \quad \text{and}$$
$$y(r,\theta) = (1-r)y_p(\theta) + ry_j(\theta)$$

where $I(x,y)$ is the iris region image, (x,y) are the original Cartesian coordinates, (r,θ) are the corresponding normalized polar coordinates, x_p , y_p and x_i , y_i are the coordinates of the pupil and iris boundaries along the θ direction. The rubber sheet model takes into account pupil dilation and size inconsistencies in order to produce a normalized representation with constant dimensions. In this way the iris region is modeled as a flexible rubber sheet anchored at the iris boundary with the pupil centre as the reference point. The centre of the pupil is considered as the reference point, and radial vectors pass through the iris region, as shown in Figure 4. A number of data points are selected along each radial line and this is defined as the radial resolution. The number of radial lines going around the iris region is defined as the angular resolution.

The normalized pattern was created by backtracking to find the Cartesian coordinates of data points from the radial and angular position in the normalized pattern. From the 'doughnut' iris region, normalization produces a 2D array with horizontal dimensions of angular resolution and vertical dimensions of radial resolution. Another 2D array was created for marking reflections, eyelashes, and eyelids detected in the segmentation stage. In order to prevent non-iris region data from corrupting the normalized representation, data points which occur along the pupil border or the iris border are discarded.

3.4 Feature Encoding

3.4.1 Gabor Filters

The 2D normalized pattern is broken up into a number of 1D signals, and then these 1D signals are convolved with 1D Gabor wavelets. The rows of the 2D normalized pattern are taken as the 1D signal, each row corresponds to a circular ring on the iris region. The angular direction is taken rather than the radial one, which corresponds to columns of the normalized pattern, since maximum independence occurs in the angular direction. As shown in Figure 5.

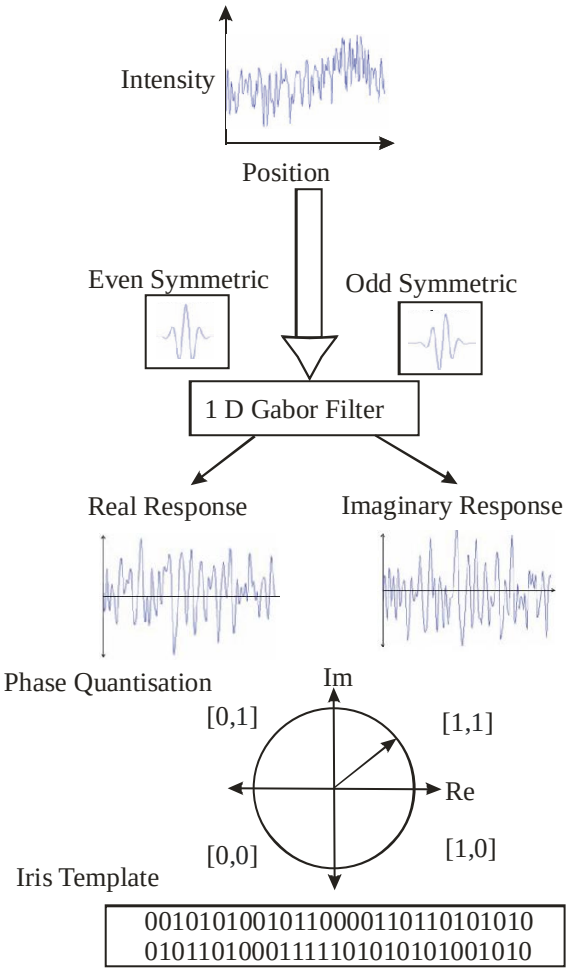

Figure 5: Feature Encoding process using Gabor Filters

The intensity values at known noise areas in the normalized pattern are set to the average intensity of surrounding pixels to prevent influence of noise in the output of the filtering. The output of filtering is then phase quantized to four levels using the Daugman method, with each filter producing two bits of data for each phase. The output of phase quantization is chosen to be a grey code, so that when going from one quadrant to another, only 1 bit changes. This will minimize the number of bits disagreeing, if say two intra-class patterns are slightly misaligned and thus will provide more accurate recognition. The feature encoding process is illustrated in Figure 5. The encoding process produces a bitwise template containing a number of bits of information, and a corresponding noise mask which corresponds to corrupt areas within the iris pattern, and marks bits in the template as corrupt. The total number of bits in the template will be the angular resolution times the radial resolution, times 2, times the number of filters used.

3.5 Barcode Generation

Bar codes are like a printed version of the Morse code. Different bar and space patterns are used to represent different characters. Sets of these patterns are grouped together to form a "symbology". There are many types of bar code symbologies each having their own special characteristics and features [1]. Most symbologies were designed to meet the needs of a specific application or industry. We take the binary template of the iris and form an equivalent barcode of it. The Aztec symbology is been used in the proposed system.

Aztec Code is a high density 2-dimensional matrix style bar code symbology that can encode up to 3750 characters from the entire 256 byte ASCII character set. The symbol is built on a square grid with a bull's-eye pattern at its centre. Data is encoded in a series of "layers" that circle around the bull's-eye pattern. Each additional layer completely surrounds the previous layer thus causing the symbol to grow in size as more data is encoded yet the symbol remains square. Aztec's primary features include: a wide range of sizes allowing both small and large messages to be encoded, orientation independent scanning and a user selectable error correction mechanism [1][7][10].

The smallest element in an Aztec symbol is called a "module" (i.e. a square dot). The module size and the amount of error correction are the only "dimensions" that can be specified for an Aztec symbol and both are user selectable. It is recommended that the module size should range between 15 to 30 mils in order to be readable by most of the scanners that are currently available.

The overall size of an Aztec symbol is dependent on the module size, the total amount of encoded data and also on the level of error correction capacity chosen by the user. The smallest Aztec symbol is 15 modules square and can encode up to 14 digits with 40% error correction. The largest symbol is 151 modules square and can encode 3000 characters or 3750 numeric digits with 25% error correction.

Once the barcode is formed, it is stored in the database. For the test data, once again the barcode is generated using above described symbology and this test data is matched with the reference data from the database.

An example for barcode of the bull's-eye pattern is shown in the following Figure 6.

Figure 6 : 2D Barcode

3.5.1 Barcode Generation Algorithm

The sequence of steps used to convert the 9600-bit binary template, which is the Iris code, into a 2D barcode is:

1. Generate a 13*13 finder structure that includes a center square and a plurality of nested squares having centers that approximately coincide with the center square. This constitutes the center part of the proposed barcode symbol. Then, generate a symbol descriptor layer surrounding finder structure that encodes data indicating size of the symbol and length of the message encoded therein.

2. Convert the binary template into Ascii values template: Make the total number of bits to 9604 by appending four 0's(in order to be divisible by 7). Then, to convert into ascii, read 7bits at a time , and convert into an ascii

character, and write them to an output file. This way we get 1372 ascii characters[1].

3. Convert the Ascii values into values specified by AZTEC symbology [1]. First store the table. Then take ascii values from the previously stored file and match them with values from table and store into another file. Again we get 1372 values.

4. Convert the values again to binary form for second level Encoding: Then convert these values again to binary bits, with 5 bits maximum and store into another file. Here, we get varying number of bits.

5. Convert the binary data into 10-bit codeword in order to encode them into the 2D Barcode: First, append extra bits if required, to make the total no of bits a multiple of 10. Then, check whether total no of bits/10 (ex: 6180/10=618) is an even number, if not append 10 more bits, to make it even. Then, read each 10-bit codeword and convert it to a decimal number and write it to a file. We get varying number of decimal numbers (need to convert to decimal for RS encoding).

6. Apply Reed-Solomon encoding to the decimal values to add error checking and generate a template of 7200 bits totally: Read the decimal numbers and apply RS encoding, then convert the decimal numbers to binary bits and store separately. we get 7200 bits constant for any iris.(we chose 7200 as it is closest to 6860, maximum of 1372*5) This gives us an error correction up to 14% [6].

7. Encode the 7200 bits into the 2D barcode after forming the 15X15 finder structure and the Symbol descriptor: We get a 2D barcode in the form of 91X91 matrix.

3.5.2 Reed-Solomon Error Checking

Reed–Solomon (RS) codes : These codes are non-binary cyclic error-correcting codes invented by Irving S. Reed and Gustave Solomon [6]. They described a systematic way of building codes that could detect and correct multiple random symbol errors. By adding *t* check symbols to the data, an RS code can detect any combination of up to *t* erroneous symbols, and correct up to ⌊*t*/2⌋ symbols. As an erasure code, it can correct up to *t* known erasures, or it can detect and correct combinations of errors and erasures. Furthermore, RS codes are suitable as multiple-burst bit-error correcting codes, since a sequence of *b*+1 consecutive bit errors can affect at most two symbols of size *b*. The choice of *t* is up to the designer of the code, and may be selected within wide limits.

They use polynomials derived using finite field mathematics known as Galois Fields. Galois Fields comprise of a finite number of elements with special properties. Either multiplication or addition can be used to combine elements in the field. Such fields generally only exist when the number of elements is a prime number or a power of a prime number. There exists at least one element called a primitive such that every other element can be expressed as a power of this element. Data are formed into symbols that are members of the Galois Field used by the code. The size of the Galois Field determines the number of symbols in the code, is based on the number of bits comprising a symbol.

Aztec Codes use Reed–Solomon error correction to allow correct reading even if a portion of the bar code is damaged. When the bar code scanner cannot recognize a bar code symbol, it will treat it as an erasure [6].

3.6 Formation of the Barcode

The barcode symbology presented here embeds data in a two dimensional grid pattern or matrix, and is directed more particularly to a 2D matrix symbology in which data blocks are concatenated in a sequentially readable spiral-like pattern having a beginning and end which can be identified quickly and uniquely with respect to a centrally located finder pattern.

In the preferred embodiment the symbology includes a finder structure and a symbol descriptor structure which together lie at and form the core of the bar code symbol. By virtue of its simple geometry and easy recognizability the finder structure allows the read circuitry to determine both the center of the barcode symbol and the axes of orientation thereof with respect to the reader. By virtue of its encoded data content the symbol descriptor structure allows the reader to determine the size of the symbol and the length of the message encoded therein. Also included within the core of the symbology is an orientation structure including a set of orientation blocks that contain codes which indicate, with respect to the structure, where should the data encoded in the symbol has to begin. Thus the finder structure comprises of a framework which contains within itself all of the data necessary to characterize the beginning point and length of the message encoded within the barcode symbol.

The symbology also includes a reference structure which comprises of easily recognizable grids that includes a plurality of linear arrays of reference elements having longitudinal axes that are oriented in parallel with one or more segments of the finder structure. The parts of this reference grid extends from within the finder structure to the outermost boundaries of the barcode and provide a Cartesian frame of reference that allows the location of any part of the symbol to be accurately read.

The symbology also includes a data structure that includes a plurality of data blocks which are organized into string having one end that is located in a predetermined position with respect to the core structure. All message data, and all check or error correction data is encoded as combinations of black and white squares (1's and 0's respectively) that are positioned within these data blocks. Each of these data blocks, in turn, includes a plurality of component blocks, hereinafter referred to as 'dominoes', which allow the spatial or directional continuity of the data blocks to be interrupted without disrupting the ability of a barcode reader to accurately read all of the data encoded therein. It is the elimination of the need for such continuity that allows the data blocks to be formed into layers which wrap around and enclose the core structure and yet which may be read sequentially with each layer and it also allows reader to move easily from one layer to next to continue reading a message.

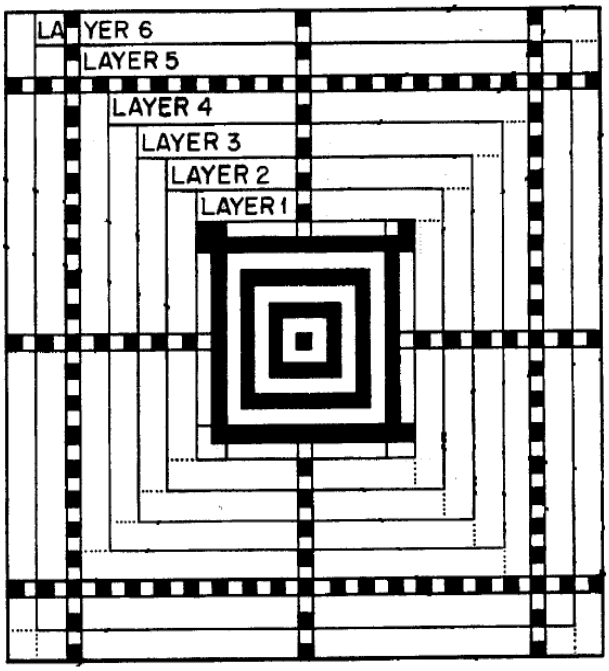

Figure 7: Structure of layers within which data is entered into the Barcode symbol.

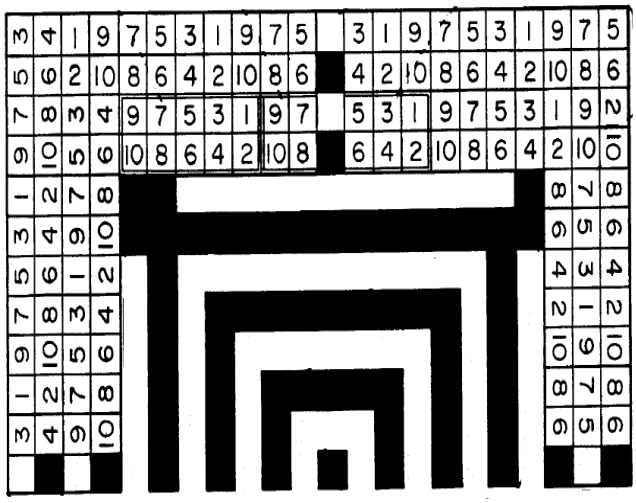

Figure 8: An enlarged fragmentary view of a Barcode which shows how data blocks are packed in.

3.7 Matching

3.7.1 Hamming Distance

For matching, the Hamming distance seems to be a good metric for recognition, since bit-wise comparisons are necessary. The Hamming distance algorithm employed also incorporates noise masking, so that only significant bits are used in calculating the Hamming distance between two iris templates. Now when taking the Hamming distance, only those bits in the iris pattern that corresponds to '0' bits in noise masks of both iris patterns will be used in the calculation [7]. The Hamming distance will be calculated using only the bits generated from the true iris region, and this modified Hamming distance formula is given as

$$HD = \frac{1}{N - \sum_{k=1}^{N} Xn_k (OR) Yn_k} \sum_{j=1}^{N} X_j (XOR) Y_j (AND) Xn_j' (AND) Yn_j'$$

where Xj and Yj are the two bit-wise templates to compare, Xn_j and Yn_j are the corresponding noise masks for Xj and Yj, and N is the number of bits represented by each template.

3.8 Interface

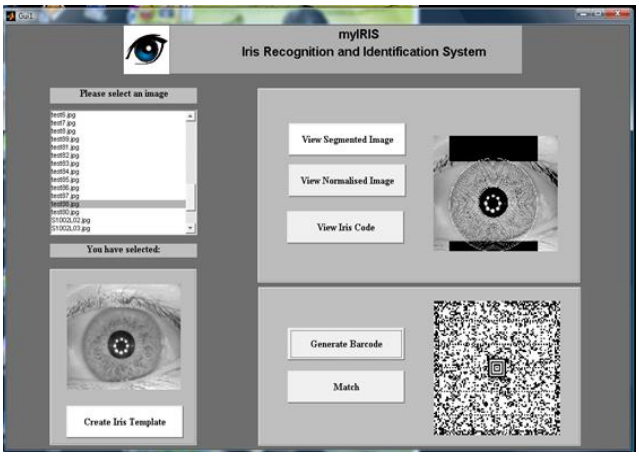

Figure 9: Generation of barcode and matching.

4. EXPERIMENTAL DATA AND RESULT ANALYSIS

The key objective of an iris recognition system is to be able to achieve a distinct separation of intra-class and inter-class Hamming distance distributions. With clear separation, a separation Hamming distance value can be chosen which allows a decision to be made when comparing two templates. If the Hamming distance between two templates is less than the separation point, the templates were generated from the same iris and a match is found. Otherwise if the Hamming distance is greater than the separation point the two templates are considered to have been generated from different irises [7].

We have conducted an experiment and the analysis carried out for 10 different images and about 10-13 samples of each image. Total comparison is about more than 100 images.

Table 1: Hamming distances between different barcode images.

Image	Hamming Distance (HD) of image I with image j									
i/j	**1**	**2**	**3**	**4**	**5**	**6**	**7**	**8**	**9**	**10**
1	0	0.3199	0.3139	0.3257	0.3103	0.3122	0.3187	0.3114	0.321	0.3224
2	0.3103	0	0.3199	0.3078	0.318	0.3134	0.3177	0.3073	0.3123	0.3188
3	0.3122	0.3169	0	0.3147	0.3166	0.3134	0.3203	0.3174	0.3196	0.3206
4	0.3187	0.3258	0.3253	0	0.3177	0.3203	0.314	0.3251	0.3288	0.3308
5	0.3114	0.3215	0.3113	0.3302	0	0.3073	0.3174	0.314	0.3225	0.3199
6	0.321	0.3201	0.3225	0.3247	0.3123	0	0.3196	0.3288	0.3225	0.3231
7	0.3224	0.3286	0.3327	0.3315	0.3188	0.3206	0	0.3308	0.3199	0.3231
8	0.3199	0.3231	0.3292	0.3199	0.3169	0.3258	0.3215	0	0.3201	0.3286
9	0.3139	0.3231	0.3347	0.3078	0.3147	0.3253	0.3113	0.3225	0	0.3327
10	0.3257	0.3292	0.3347	0.318	0.3166	0.3251	0.3302	0.3247	0.3315	0

Table 2 : Hamming distances between barcode image and its own samples

Image	Hamming Distance (HD) of image i with sample j													
i/j	**1**	**2**	**3**	**4**	**5**	**6**	**7**	**8**	**9**	**10**	**11**	**12**	**13**	**14**
1	0	0.3071	0.295	0.312	0.3068	0.2968	0.299	0.3061	0.3035	0.3017	-	-	-	-
2	0.3113	0	0.3088	0.3125	0.314	0.3044	0.3166	0.3066	0.3212	0.3167	-	-	-	-
3	0.3106	0.3212	0	0.3076	0.3084	0.321	0.3184	0.3112	0.3103	0.3152	-	-	-	-
4	0.3186	0.311	0.3166	0	0.3124	0.3161	0.3131	0.317	0.3233	0.3146	0.3234	-	-	-
5	0.3211	0.3217	0.3239	0.3145	0	0.3181	0.3178	0.3172	0.323	-	-	-	-	-
6	0.3143	0.2776	0.2841	0.3145	0.2831	0	0.315	-	-	-	-	-	-	-
7	0.3122	0.3236	0.3113	0.3165	0.3141	0.3129	0	-	-	-	-	-	-	-
8	0.3131	0.3084	0.3239	-	-	-	-	-	-	-	-	-	-	-
9	0.3205	0.3136	0.324	0.3218	0.3207	0.3102	0.318	0.3192	0	0.3267	0.3299	0.326	0.3315	0.327
10	0.3215	0.3238	0.3289	0.3205	0.3291	-	-	-	-	-	-	-	-	-

- Observing both the table's values, separation point is set to '0.3180'
- Based on this separation point, following parameters are been determined.

1. AR- Acceptance Ratio is the Number of samples of the image that are accepted correctly/Total number of samples.
2. FRR- False Rejection Ratio is the Number of samples of the image that are rejected falsely/Total number of samples.
3. FAR-False Acceptance Ratio is the Number of different images that are accepted falsely/ Total number of images.
4. RR- Rejection Ratio is the Number of different images that are rejected correctly/ Total number of images.

Table 3 : Result Analysis

Sl. No	Parameter	No. of Samples	Total Samples	Percentage of Result
1	AR	46	78	58.90%
2	FRR	32	78	41.10%
3	FAR	31	90	33.34%
4	RR	59	90	66.66%

5. CONCLUSION

From the above calculations, we can conclude that the proposed system is about 60% efficient in accepting valid images and about 67% efficient in rejecting invalid images.

6. ACKNOWLEDGMENTS

The authors wish to thank Miss. Preeti Pai, Miss. Tejaswini A.,
and Miss. Sneha Dinkar Rao for their implementation support. And also CASIA for providing the iris database. The shared CASIA Iris Database is available on the web.[2].

7. REFERENCES

[1] Andrew Longacre, Jr. and Robb Hussey, Two dimensional Data Encoding Structure and Symbology for Use with Optical Fibres, United States Patent, Patent Number: 5591956, May 15, 1995.

[2] Chinese Academy of Sciences — Institute of Automation (CASIA) Iris Database http://www.cbsr.ia.ac.cn

[3] J.Daugman, How iris recognition works. Proceedings of 2002 International Conference on Image Processing, Vol. 1, 2002.

[4] J. Daugman. High confidence visual recognition of persons by a test of statistical independence. IEEE Transactions on Pattern Analysis and Machine Intelligence, Vol. 15, No. 11,1993.

[5] J. Daugman. Biometric personal identification system based on iris analysis. United States Patent, Patent Number: 5,291,560, 1994.

[6] Joel Sylvester, Reed Soloman Codes, January 2001.

[7] Libor Masek, Recognition of Human Iris Patterns for Biometric Identification, The University of Western Australia, 2003

[8] N. Tun. Recognising Iris Patterns for Person (or Individual) Identification. Honours thesis, The University of Western Australia. 2002.

[9] R. Wildes, J. Asmuth, G. Green, S. Hsu, R. Kolczynski, J. Matey, S. McBride. A system for automated iris recognition. Proceedings IEEE Workshop on Applications of Computer Vision, Sarasota, FL, pp. 121-128, 1994.

[10] S. Sanderson, J. Erbetta. Authentication for secure environments based on iris scanning technology. IEE Colloquium on Visual Biometrics, 2000.